F61/62
Nuclear magnetic resonance

FP- Universität Heidelberg

Anna-Teresa Daum und Tabita Bomhard

27. September 2023

Inhaltsverzeichnis

1 Introduction

1.1 Motivation

Nuclear magnetic resonance (NMR) spectroscopy is a modern tool for medical imaging and the identification of chemical substances. The method uses spin relaxation times in strong magnetic fields to do spectroscopy on the molecules of interest. Here we represent our results of our measurements on the F61/62 NMR measurement apparatus. We started out investigating different measurement techniques to obtain the relaxation times T1 and T2. A high frequency pulse was then used to determine the frequency spectrum of different molecules in relation to Tetra-Methyl-Silan. With these results we were able to identify the five given substances making use of shifts in the larmor frequency. At last we did images of different objects to obtain their inner structure.

1.2 Basics of NMR

Every nuclei with a spin S (nonzero) shows a magnetic dipole moment in dependence of the gyromagnetic moment γ:

$$\mu = \hbar \cdot \gamma \cdot S \tag{1}$$

In our measurment we are looking at protons and therefore: $\gamma = 2.6752 \cdot 10^8 \frac{1}{T \cdot sec}$.

A nucleus's magnetic dipole moment therefore interacts with an external magnetic field B_0 to the extend that the spin aligns with the B-field (anti-)parallelly. The interaction energy for this is :

$$\Delta E = -\mu \cdot B_0 \tag{2}$$

For a sample with N protons the populations occupying parallel or antiparallel states are defined by a Boltzmann distribution. A macroscopic magnetization M_0 is caused by more protons being in the parallel state, because the parallel state is energetically more favorable. This magnetization is defined by:

$$M = \frac{1}{V} \sum \mu_i \tag{3}$$

$M_0 \parallel B_0$ is the ground state, which has minimized energy. In general, arbitrary directions relative to the external field are possible. Splitting M_0 into a parallel $M_\parallel$ and orthogonal $M_\perp$ part in consideration of the external field. Such a state will asymptotically dissipate its excitation energy in form of an characteristic time scale. The interaction between the external magnetic field B_0 and the magnetization M results in a torque τ acting on the magnetization:

$$\tau = M \wedge B_0 \tag{4}$$

This torque is zero if the magnetization and the magnetic field are parallel, as is the case for the ground state magnetization M_0 and also $M_\parallel$ and therefore also antiparallel in an external static field.

So the torgue is only acting on $M_\perp$, which then precess around B_0 with the angular Larmor frequency ω_L:

$$\omega_L = \gamma B_0 \tag{5}$$

A magnetization M transverse or $M_\parallel$ antiparallel to B_0 can be generated by applying a high frequency pulse with ω_{HF} to the ground state magnetization M_0.

The spins are determined by a time-dependent Magnetic field $B_1(t)$ excited or deflected. A coil is placed in the magnetic field. The oscillating Magnetic field of the nuclei induces a current and thus a signal, a pulse.

1.3 Relaxation time

Important for this experiment are two different types of relaxation times: T1, the so called spin-lattice relaxation time and T2 the spin-spin relaxation time.
T1: On the one hand, the spin-lattice relaxation time T1 is measured using a 180° pulse which causes an antiparallel magnetization $M_{\parallel}$ to B_0. Because this action lags a measurable signal as described in the basics, a 90° pulse is induced at $t = \tau$ to get a transverse recognizable magnetization.

T2: On the other hand, the spin-spin relaxation time is measured with the spin echo method. A 90° pulse is applied to the sample at t = 0. The transverse magnetization $M_{\perp}$ will rotate around B_0 with ω_L. Due to an only approximate homogeneous magnetic field, the protons posses different ω_L. Thus they develop a difference of phase, which can be reversed by applying a 180° pulse at a time $t = \tau$, leading to the same phase at $t = 2\tau$. The other method is called Carr-Purcell sequence and is same as the spin echo method, but repeated. Therefore applying a 180° pulse at uneven times τ to receive a phase coherence at the following even times τ afterwards. The more often this is done the more precise the relaxation time gets.
With help of the bloch-equations we get:

$$M_{\parallel} = M_0(1 - 2e^{\frac{-t}{T_1}}) \tag{6}$$

and

$$M_{\perp} = M_0 e^{\frac{-t}{T_2}} \tag{7}$$

1.4 Chemical shift

The essential for measuring the chemical shift is the diversity of molecule structures, unfolding different Larmor frequencies. This frequency is determined by a total magnetic field B_{tot} which comprises a shielding contribution:

$$\delta B = -\sigma B_0 \tag{8}$$

and the external field B_0 .The formula is formed due to a characteristic proportionality shielding factor σ of the electron orbitals of the molecule and each of its nuclei.Thus, the Larmor frequecy can be used as

$$\omega_i = \omega_L(1 - \sigma_i) \tag{9}$$

with ω_i as the frequency modified by the chemical shift. In addition with a reference substance (e.g. Tetramethylsilane TMS) substances can be identified with their chemical shift δ_i.

$$\delta_i = \sigma_i - \sigma_{TMS} = \frac{\omega_{TMS} - \omega_i}{\omega_L} \tag{10}$$

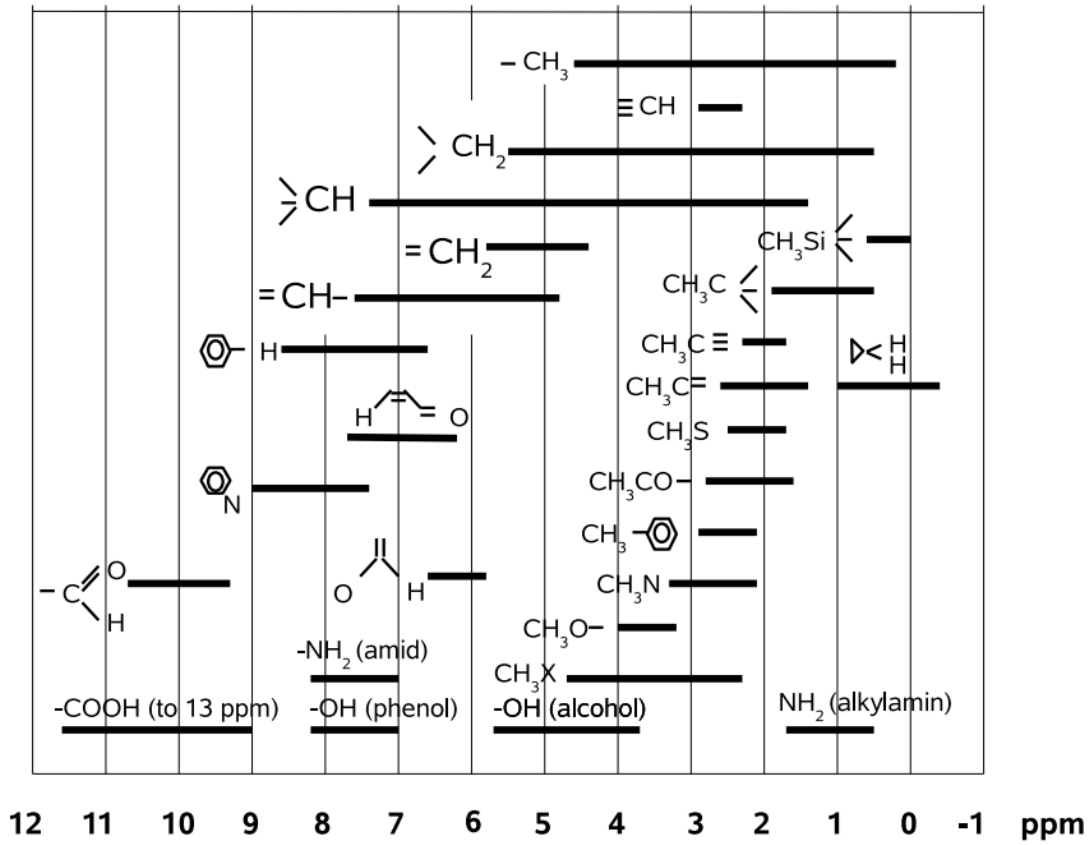

Chemical shifts i of compounds relative to TMS

1.5 Imaging with NMR

Using a linear gradient field, hence a position dependant magnetic field superimposed by B_0 Thus one can link a specific frequency measured a specific position. The static B_0 field points here in the z direction. There are two mathematically equivalent methods for one-dimensional imaging. Once frequency coding and once the phase coding. The NMR signal results from the fourier transformation of orthogonal magnetization. With frequency coding the signal is at $t_n = n \cdot \Delta t$ recorded. This results in a set of data points. With phase coding, the phase varied by a gradient field. The strength of this field is increased bit by bit.

In two-dimensional imaging, a layer is also selected in which all nuclei have the same Larmor frequency. In comparison to the environment, which is not stimulated,there is a phase difference. Two-dimensional imaging is best done using the following graphic be illustrated.

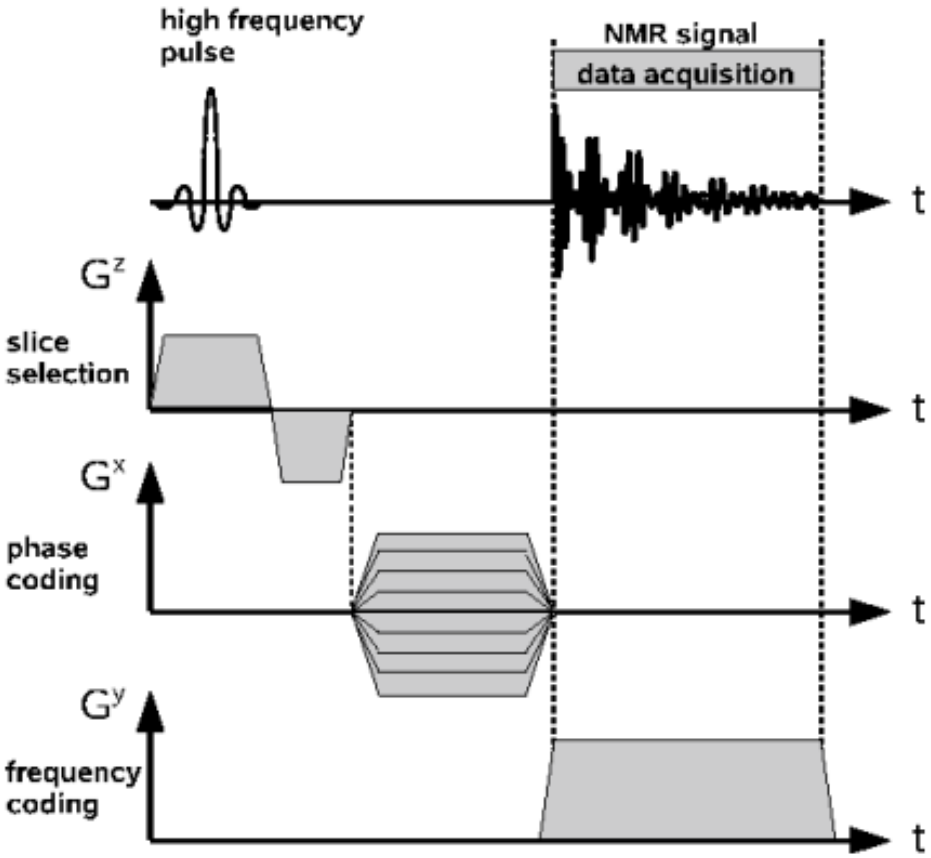

Timing diagram for the two dimensional Fourier method

First you switch a high-frequency pulse in a specific slice (z-direction).The described phase difference of this layer to the surroundings is lifted by a refocusing gradient. Then you use the phase coding in the x direction and the frequency coding in the y direction to generate a two-dimensional image.

2 Experimental setup

Two separate setups are used. The first consists of a p20 electronic unit and a p20 magnet, which are connected to an oscilloscope and a PC with LabVIEW. In order to get a better measurment of the substances, these are set in rotation with help of pressured air that goes to a small gear directly to the testtube. The second setup for the MRI imaging,represents a Bruker minispec mq7.5, which is directly connected to a computer. The device is shown in Figure 4. The samples (test tubes with a liquid or other object in it), can be placed in the center of the device's coil assembly. The image data is loaded onto a connected computer and can be viewed in another LaVIEW program.

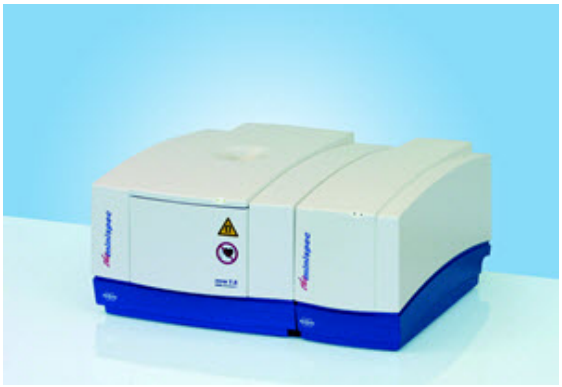

Abbildung 1: Bruker minispec mq 7.5

3 Experimental procedure

Calibration First, the p20 unit is connected directly to the oscilloscope in order to monitor the pulse curve.By trying it out you can find the controls for the pulse duration and the pulse interval τ .

The pulse duration is now calibrated for reaching the maximum amplitude of the oscillating atoms at a 90°pulse. Conversely, the minimum amplitude is sought for the 180° pulse. To do this, the GD600 sample is placed in the magnetic field and the controls are adjusted so that the maximum and minimum signals are received. The controls are not changed for the rest of the experiment.

Various methods of nuclear magnetic resonance:Relaxation times As already explained, in this part we measured T_1 and T_2 of Gd500/600. We used the spin echo method and the Carr-Purcell method for the measurement of T_2. For spin echo, we varied the measurement time 2τ from 40-400 ms. With the Carr-Purcell method we had a difference between measurements of 20 ms and a total measurement time of about 190 ms. For the T_1 measurement we varied the measurement duration from 40-600ms.

Determination of substances using chemical shifts In this part of the experiment we looked at 5 different liquid samples. We have the samples with and without the reference substance tetra-methyl-silane (TMS). We first inserted each of these samples into the device and brought it to a high rotation speed using compressed air. The material was then stimulated with a high-frequency pulse to record a frequency spectrum. We made sure that the spectrum was as complete as possible in the range from 0Hz to 1kHz in which our spectrometer can measure. We then evaluated the peaks in ppm in the LabVIEW program. This allowed us to compare the samples with and without TMS to assign the samples to the 5 given substrates and their specific chemical shifts.

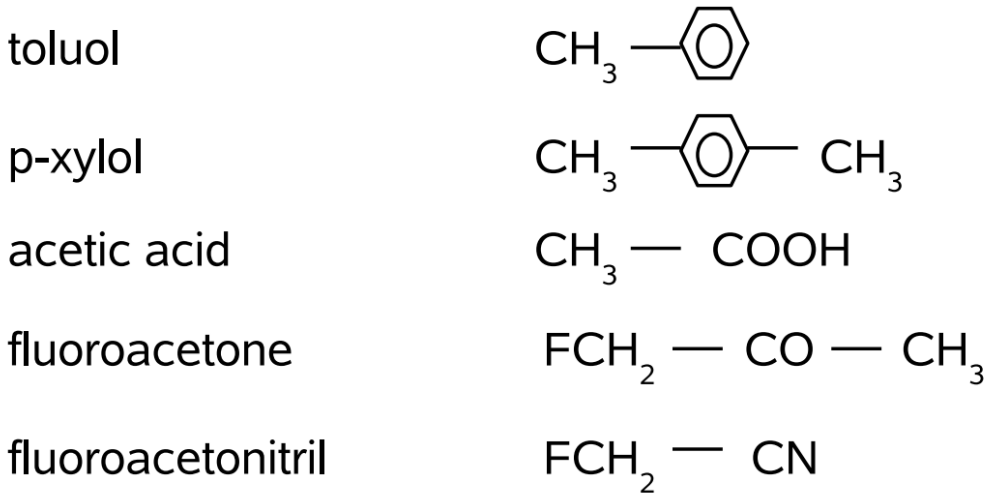

Abbildung 2: Five substances for identification

Imaging methods using nuclear magnetic resonance We used different samples for the 1D and 2D measurements. For the 1D measurement these were various oil-filled test tubes and a Teflon structure in oil. We also allowed the oil to seep into the sand and recorded the structure after many time steps. For the 2D recordings, we recorded various objects such as chili peppers, selery and a peanut in different layers.

4 Results

4.1 Relaxation time

You can see our measured results of the different relaxation times in the following table1:

Probe	T_1	T_2 Spin-Echo	T_2 Carr-Purcell	σ-Abweichung T_2
Gd500	155.8+-1.1ms	120.6+-1.9ms	100.4+-1.0ms	9.4
Gd600	170.4+-1.4ms	125.8+-2.0ms	115.0+-0.8ms	5

Tabelle 1: measurement results of relaxation times

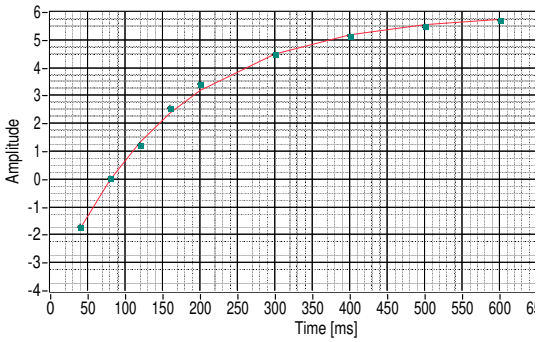

Abbildung 3: T1-Gd500

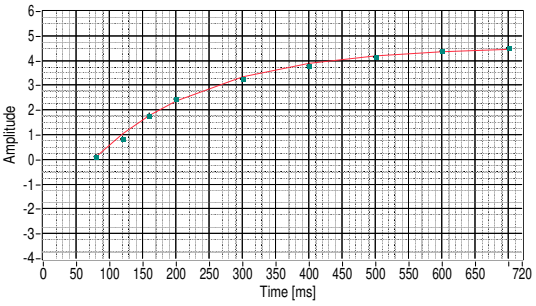

Abbildung 4: T1-Gd600

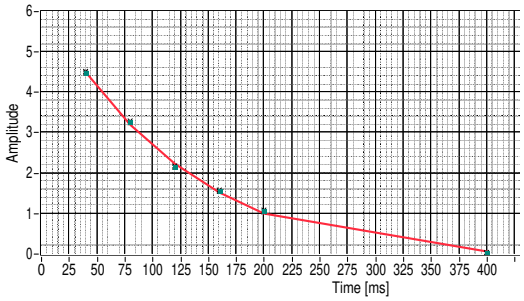

Abbildung 5: T2-SE-Gd500

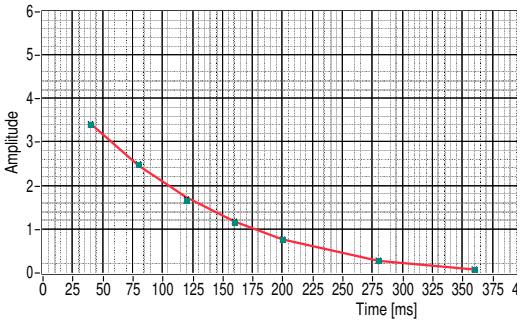

Abbildung 6: T2-SE-Gd600

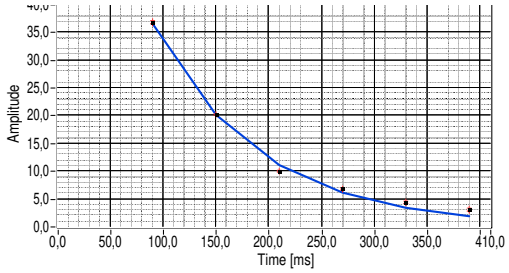

Abbildung 7: T2-CP-Gd500

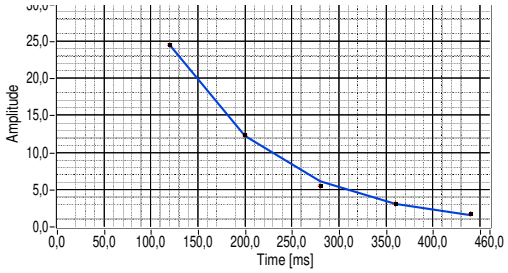

Abbildung 8: T2-CP-Gd600

The graphics show us the expected shape of the function of equation 6 and 7. If we look at the table and compare the relaxation times, we can see that the times, measured with Gd500 are smaller than the Measurements with Gd600. This is due to the concentration of gadolinium. While in the Gd500 sample there is one part gadolinium to 500 parts water, the ratio for the Gd600 sample is 1:600. Gd500 therefore has a higher gadolinium concentration as Gd600. The higher concentrations reduce the mobility of the molecules in the sample. This causes less interactions between the protons themselves and the magnetic field. The gadolinium also has a magnetic moment, which can interact with the magnetic field independent in addition to the magnetic moments of the protons of the water. Thus the shorter relaxation times in the Gd500 sample.

When measuring T_2, we observed large deviations between the measurements using the spin echo method and the Carr-Purcell method. The difference between the two methods is 9.4σ for Gd500 and 5σ for Gd600. It is expected that the Carr-Purcell method yields better results than the spin echo method, which systematically overestimates the relaxation time. In our case the time rankings are not consistent with our theory. The Carr-Purcell values are smaller than the times measured with the spin-echo method. The reason for that lies in our pulse calibration we did before starting with the measurements. Because of the inhomogeneity of the B-field we couldnt calibrate the 180° Pulse that way, in which $M_\perp = 0$. It should be noted that the spin-echo method also has significantly higher systematic errors than the Carr-Purcell method. This poorer quality is due, among other things, to the significantly shorter measurement time and these errors were not determined in our measurement. Another source of error was a shift in the Lamor frequency due to the change in the magnetic field, which means that the entire frequency spectrum was not always recorded perfectly, which means that the Fourier transform can no longer be used well for the measurment.

Additionally it is expected to see a higher value for T1 than for T2, as the longitudinal or parallel relaxation has one less degree of freedom than the transversal or perpendicular relaxation, thus the higher relaxation time. This theory we can confirm with our results. Another reason for the higher time is that it has only one process while for T2 we have two independent processes.

4.2 Chemical shift

For identifying different substances we used a reference substance(TMS) and calculated the frequency difference in ppm between the additional peaks.Before we made considerations based on the formulas how many peaks we could expect for the different substances. Then we could read out most of the substances with help of the graphic in the script and their formulas.

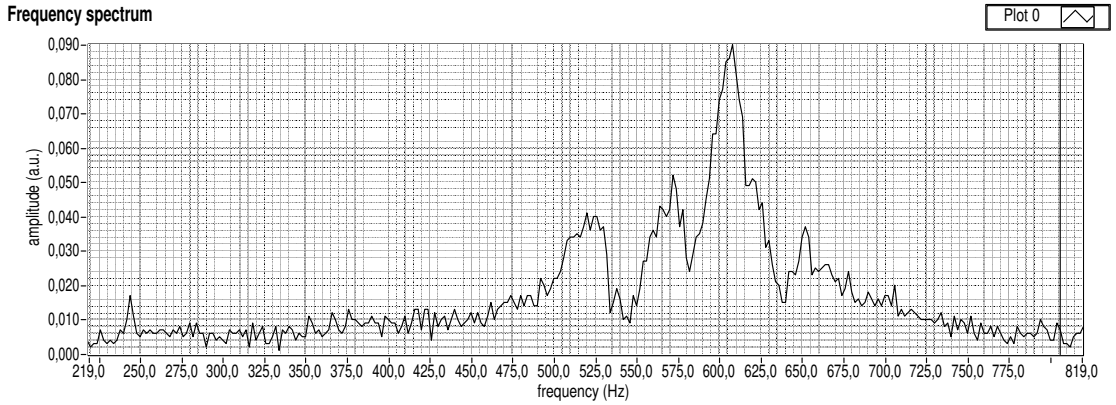

Abbildung 9: A_+

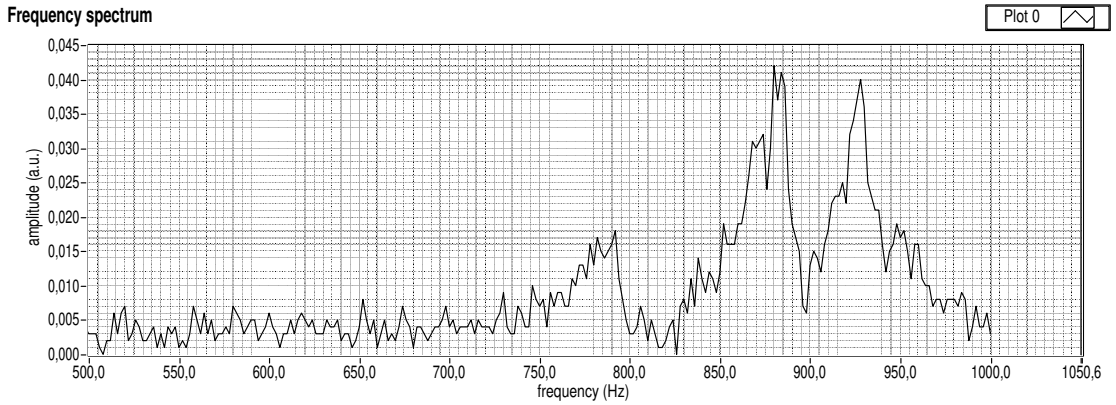

Abbildung 10: B_+

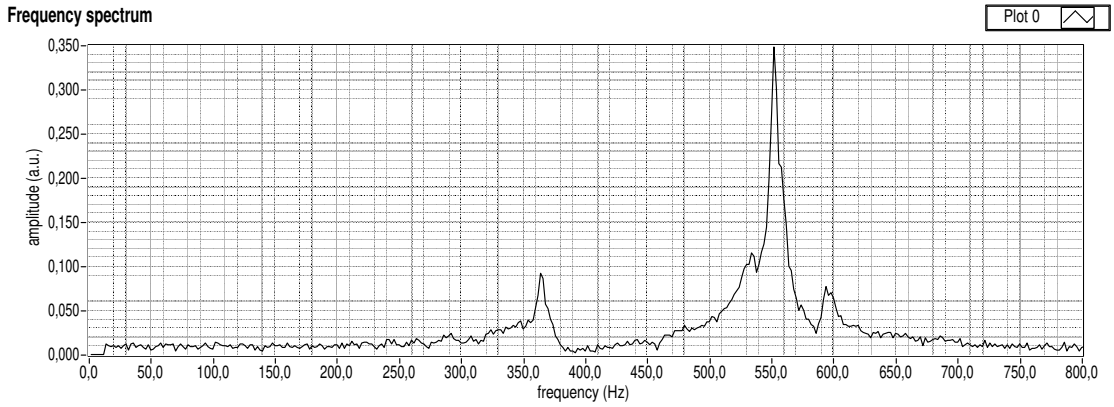

Abbildung 11: C_+

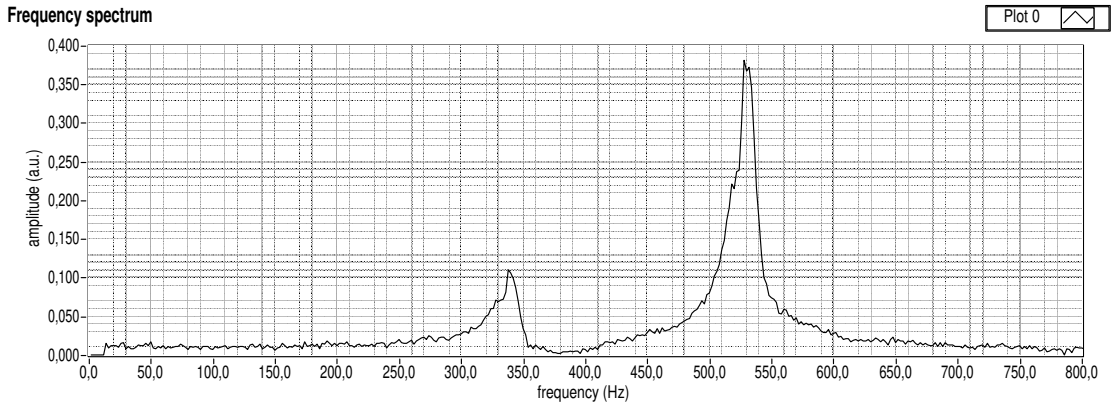

Abbildung 12: C

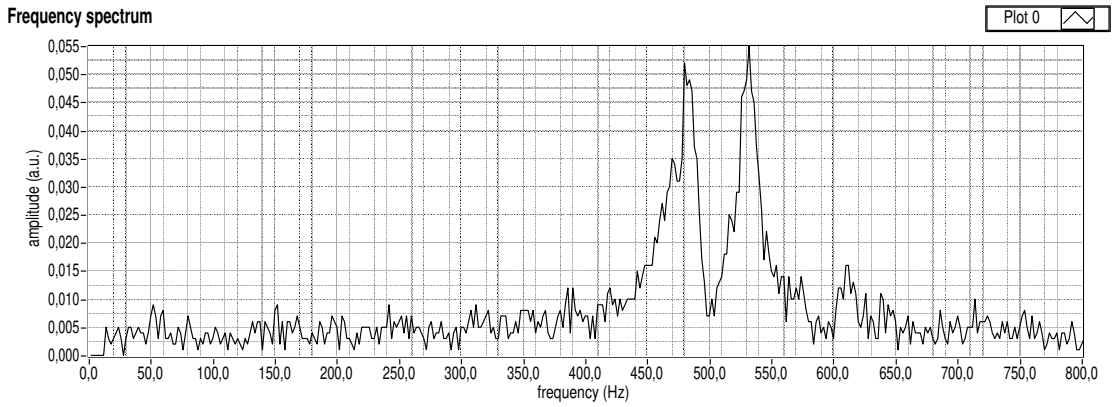

Abbildung 13: D_+

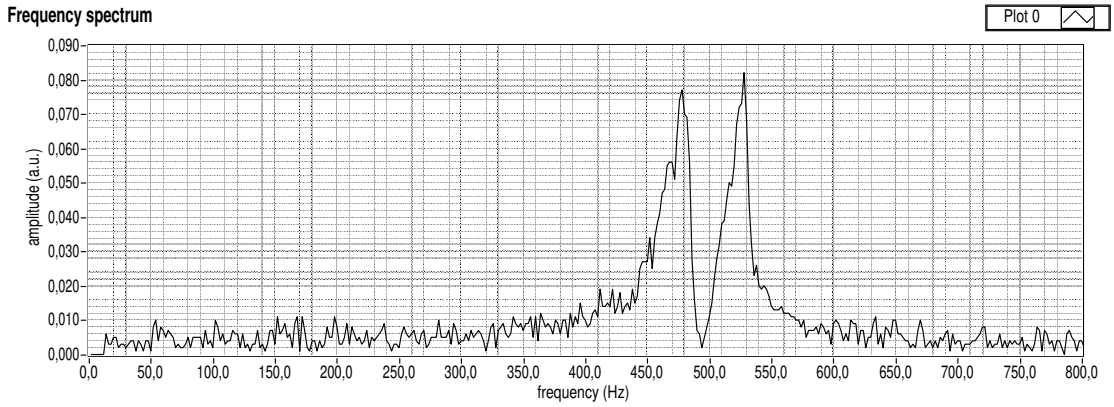

Abbildung 14: D

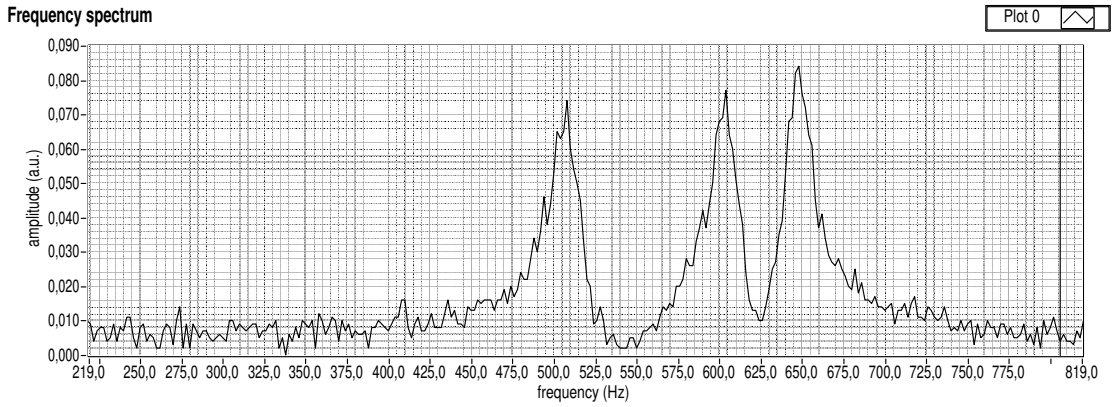

Abbildung 15: E_+

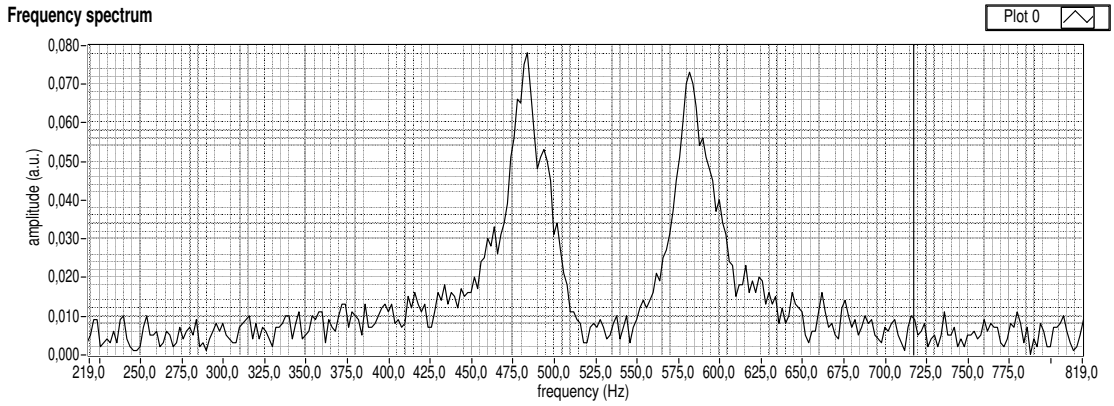

Abbildung 16: E

Probe	ref.	ppm1	ppm2	ppm3	Δ_1 [ppm]	Δ_2 [ppm]	Δ_3 [ppm]
A+	32.9	30.6	28.8	26.1	2.3	4.1	6.8
B+	46.9	44.5	37.3	-	2.4	9.6	-
C+	30.1	26.8	17.2	-	3.3	12.9	-
D+	30.8	26.7	24.1	-	4.1	6.7	-
E+	32.7	29.4	24.4	-	3.3	8.3	-

Tabelle 2: Messung und Zuordnung der chemical shifts relativ zum TMS peak

With help of the table in the script we can identify the different substances:

Probe	Substance
A+	fluoracetone
B+	p-Xylol
C+	acetic acid
D+	fluoroacetonitril
E+	toluol

Tabelle 3: Zuordnung der chemical

The first one(A) we could easily identify as Fluoroacetone because it is the only one with 3 peaks. It has the same chemical shifts as D, which we could therefore identify as fluoroacetonitril. These two peaks come from the Fluor of FH_2. The energy is $E = \hbar \cdot \omega_L$ because of an additional magnetic moment, which results in one line splitting in two lines. Fluoroacetone has a third line because of the proton of CH_3. C we can single out because of its unique large chemical shift because of -COOH as we can see in the graphic in the introduction. Probes B and E have similar chemical shifts, so that we cannot use the table for identifying. We have to take a look at the intensity of the peaks. While in the frequency spectrum of B we can see that the second peak is twice as high as the first one. In comparison to E, there are two peaks with the same height. Since p-Xylol has two CH_3 we can conclude that this is probe B and tuluol with one CH_3 is probe E.

4.3 Imaging

4.3.1 One dimensional imaging of Oil and Sand

First, two samples of oil with different fill levels (15 mm and 50 mm) are placed in the magnetic field and the Verticals examined.

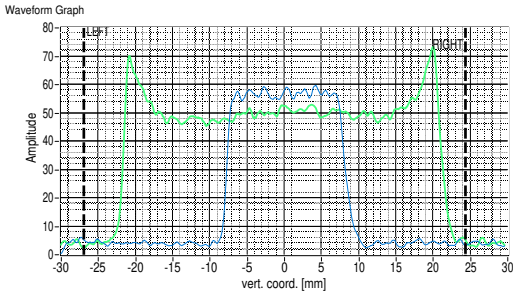

Abbildung 17: Big and small oil

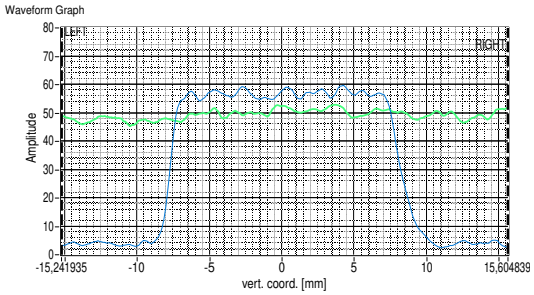

Abbildung 18: Big and small oil zoom

We can observe, that the shorter oil vial is completely visible, unlike the taller vial, which, in theory, should have given us a constant signal all along. Instead, we see bigger peaks at the ends of the signal. This is due to the fact, that the magnetic field inside the machine is not linear everywhere and especially at the edge of the measuring chamber, where it differs quite a bit. That means that there is an effective zone, where the measurements are accurate, which is smaller than the measuring chamber.

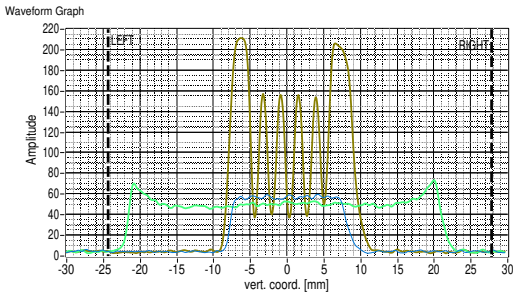

Abbildung 19: Oil with teflon bands

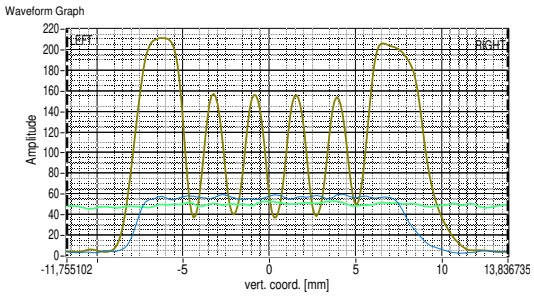

Abbildung 20: teflon zoom

The next pictures show us the signal of Oil with teflon plates in between. The missing signal in form of minimums and peaks make the teflon plates in the sample clearly visible, due to the fact that teflon does not produce a NMR signal. You can see that the image shows jagged peaks and not sharp rectangles, and the minimums are not at zero but slightly higher. That means the structure cannot be resolved precisely enough. A measuring point always contains one part oil and one part Teflon, which is how we get the jagged pattern. The peaks on the outside are larger because the area covered in oil is bigger on the bottom and top of the prob.

Finally, oil was added to a layer of sand. The leakage is recorded in the device and shown here as presented over time.

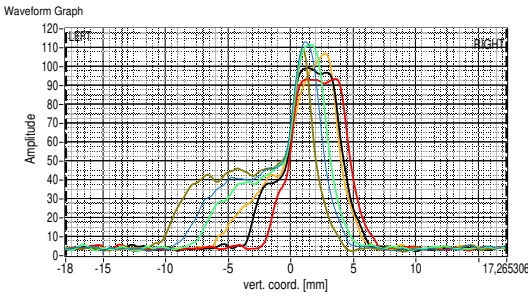

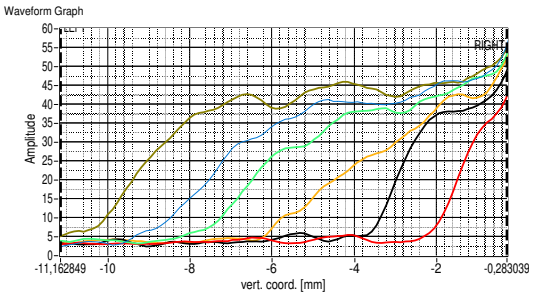

Abbildung 21: Ölsand

Abbildung 22: Ölsand 2

A concave shape can be seen after some time. This does not correspond to the diffusion curve provided and with the differential diffusion equation, which yields a convex curve for a single dimension. As can be seen in the picture, the oil spreads over time in a negative vertical direction at a decreasing rate. However, in contrast to a diffusion curve, the curve is not convex, but concave, which is why this process cannot be diffusion. This process is called percolation, which describes the movement and filtering of fluids through porous materials.

4.3.2 Two dimensional Imaging

After we made some test runs with the oil, we examined a Peanuts with the shell, a chili pepper and a stem piece of celery and in the end a small chocolate bar with nuts.

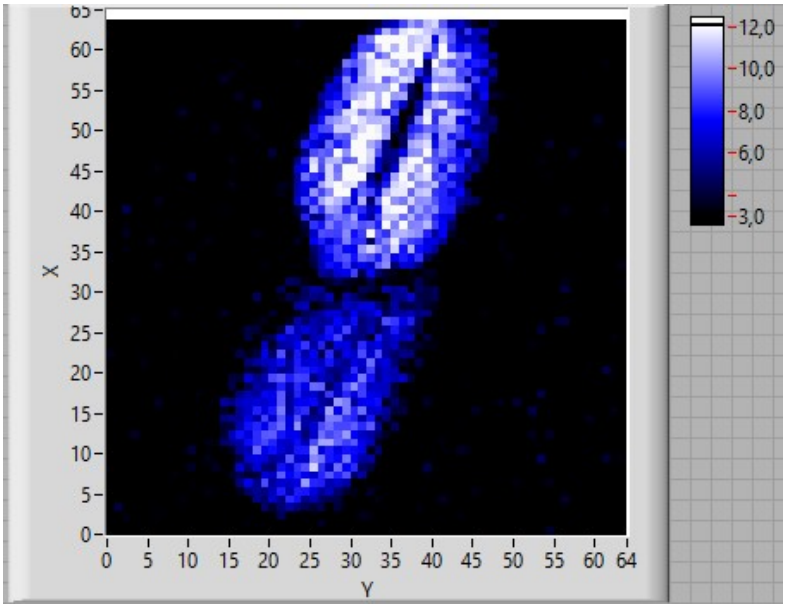

Abbildung 23: Peanut

The molecules in the shell do not emit a signal because there is no water stored in them, in contrast to the fruits. We can see the gap between the peanuts very well. Because of the fat of the peanuts we have an NMR signal and can see the structur.

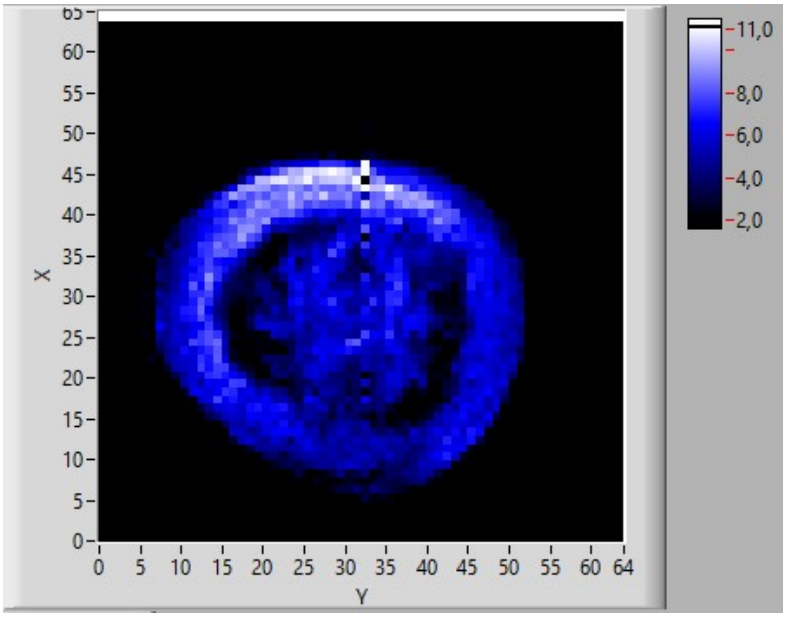

Abbildung 24: Chilli

For the chili pepper was a much higher time needed in order to see interpretable results. In the middle we can locate the seeds.

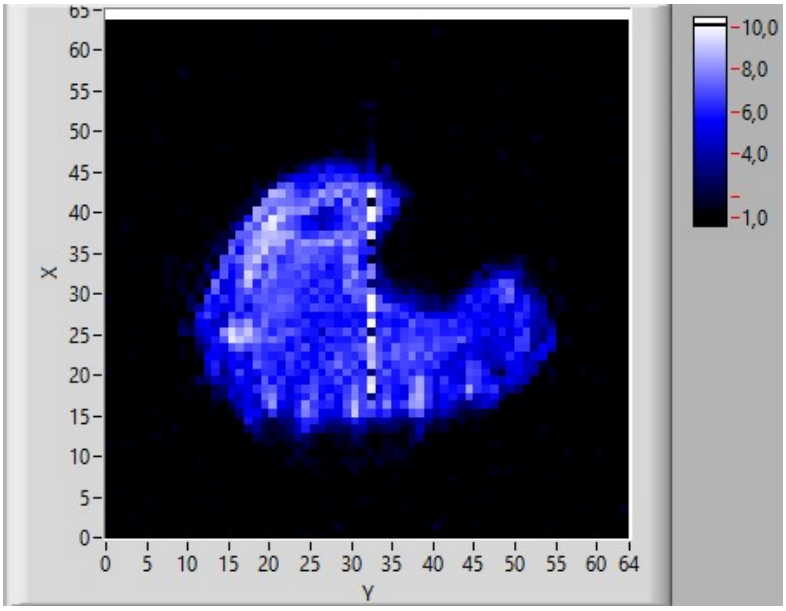

Abbildung 25: Sellery

The sellery was a little harder to examine, because it was already dry at some points. If the sellery would be still fresh, we should have seen holes with water here. However, these can be only slightly

interpreted in this picture. In the left corner, where it is more white we can assume that there was more water.

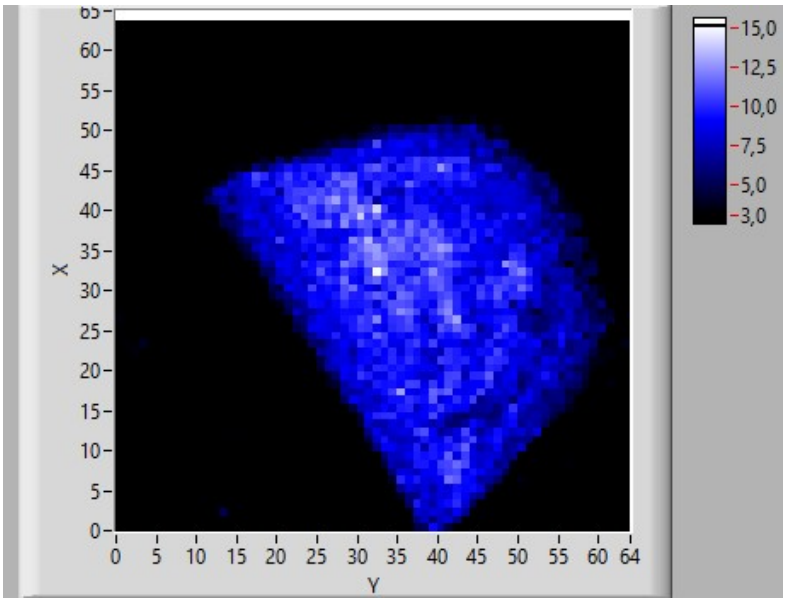

Abbildung 26: chocolate

In this last picture we looked at a small chocolate bar. We can identify a little bit of structure in the middle, which are probably the nuts.
For most objects that can reveal a thinner inner structure, the guideline is the time. The longer the measuring time, the better and more informative the image.

5 Summary and discussion

In this experiment, the functionality of nuclear magnetic resonance spectroscopy was examined. First the relaxation times T1 and T2 of samples with different concentrations were measured. Afterwards the signals of a sample were averaged to obtain the respective Larmour frequencies. On another device, individual areas of the sample can be viewed using a magnetic field gradient, so that an MRI image could be made.

In the first part, the principle of NRM was tested in a p20 magnet on various samples. After the device was calibrated, the relaxation time of two different gadolinium concentrations could be determined. This was done using the spin echo method and the Carr-Purcell method. We could not determine major differences between the two methods. Only the error is a little smaller with the Carr-Purcell method. This method should too be more accurate, as the phase differences are reduced with each 180° pulse (in the CD method, this pulse is carried out several times in a row) and thus a more uniform Larmour frequency results. In our results we can had a higher accuracy with the spin-echo method, which is caused by the inhomogeneity of the B-field.
Next, various unknown samples were put into the magnet, from which the frequency spectrum of the emerging signals was displayed. When measuring the chemical shifts, we were able to assign the samples relatively clearly. We rotated the samples with air pressure to minimize inhomogeneities in the magnetic field, but of course there still can be left a small inhomogeneity which influences our measurment. We sometimes had problems with noise, but these could be resolved in a second measurement.
One source of error in the measurements could be that we had to adjust the Lamorfrequency manual with a knob on the experiment box. It changed vary fast over time, so that it can be that sometimes it wasnt in the correct position.

In the second part, the Bruker Minispec was used, a more modern device that can be used to take MRI images of samples. The first step was to make an one-dimensional, vertical measurement of the intensity in an oil sample. First, a picture was taken at a full stand of 15mm, witch resulted in a a rectangular Shape with sharp edges resulted. That was meeting our expectations. The same recording was made at 50mm full level. The width of the rectangle has logically increased from around 15mm to around 50mm. In addition, the intensity at the edges of the sample is now increased significantly. This is because the magnetic field in the device is not linear everywhere. It varies particularly at the ends of the measuring chamber. The ends of the sample are therefore in an area in which the measurement is no longer accurate because the effective measuring range is smaller than the entire measuring chamber. The measurement of Teflon layers in oil is also intuitively clear: since the Teflon layers cannot be excited magnetically, the amplitude drops at these points, so that a wave-shaped diagram is created. There is no rectangle shape anymore because the resolution isnt high enough. Finally, a test tube is filled with sand and covered with a layer of oil. The measurement is repeated at time intervals while the oil slowly seeped through the sand. This can be seen very clearly in the resulting diagram, as the maximum mum slowly becomes narrower, while to the left of it an increase in amplitude becomes visible. The later a picture is taken, the further this “comb” extends to the left.
Now it was finally time to take two-dimensional images. At the oil test a relatively homogeneous area could be seen, which when cut horizontally was a circle, and when cut vertically it was a rectangle with small notches at the top and bottom. The notch at the bottom is most likely due to the shape of the bottom of the vessel, while the notch at the top is due to the alternating effects of the oil, which could come from the shape of the glass tube. When examining nuts, it was easy to see the fruits because the oil and water they contained is made visible through the NMR imaging. Inside the peanuts, the cavity creates a dark place in the picture. The peanut as the other objects like the chilli could be examined better with longer measurements, so the structure could be seen better.

All in all, this experiment made it possible to understand how an MRI works. While in the first part you still had to struggle a lot with the outdated device, you were able to take some very interesting shots with the Bruker, which are not visible to the naked eye.